

NAST: Non-Autoregressive Spatial-Temporal Transformer for Time Series Forecasting

Kai Chen¹ Guang Chen¹ Dan Xu² Lijun Zhang¹ Yuyao Huang¹ Alois Knoll³

Abstract

Although Transformer has made breakthrough success in widespread domains especially in Natural Language Processing (NLP), applying it to time series forecasting is still a great challenge. In time series forecasting, the autoregressive decoding of canonical Transformer models could introduce huge accumulative errors inevitably. Besides, utilizing Transformer to deal with spatial-temporal dependencies in the problem still faces tough difficulties. To tackle these limitations, this work is the first attempt to propose a Non-Autoregressive Transformer architecture for time series forecasting, aiming at overcoming the time delay and accumulative error issues in the canonical Transformer. Moreover, we present a novel spatial-temporal attention mechanism, building a bridge by a learned temporal influence map to fill the gaps between the spatial and temporal attention, so that spatial and temporal dependencies can be processed integrally. Empirically, we evaluate our model on diversified ego-centric future localization datasets and demonstrate state-of-the-art performance on both real-time and accuracy.

1. Introduction

Transformer has achieved breakthrough success in a broad variety of tasks (Carion et al., 2020; Huang et al., 2019; Liu et al., 2020), especially in Natural Language Processing (NLP), far beyond models that rely heavily on Recurrent Neural Networks (RNNs) (Vaswani et al., 2017; Brown et al., 2020; Dai et al., 2019). However, the application of Transformer for time series processing is still barely explored in the literature, where RNNs are commonly utilized in the modeling (Sagheer & Kotb, 2019; Karim et al., 2018) though showing unsatisfactory performances and im-

¹Tongji University ²The Hong Kong University of Science and Technology ³Technical University of Munich. Correspondence to: Guang Chen <guangchen@tongji.edu.cn>.

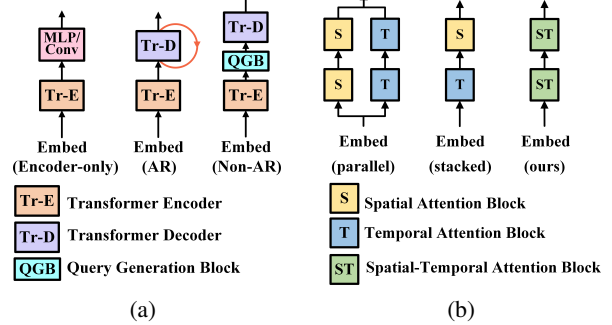


Figure 1. (a) The schematic diagram of the three decoding methods of Transformer for time series. (AR: Autoregressive; Non-AR: Non-Autoregressive; MLP: Multi-Layer Perceptron) (b) The schematic diagram of three different manners to deal with modeling spatial and temporal dependencies in Transformer architecture.

provements. Considering the acclaimed great advantages in various fields and the immense potential of surpassing RNNs, Transformer could be a desirable candidate to handle the time series forecasting problem.

However, directly transferring the power of Transformer into the time series forecasting task may be notoriously difficult due to facing serious challenges in two-folds. Firstly, the existing decoding mechanisms of Transformer for time series forecasting, as shown in Figure 1(a), are not straightforwardly applicable and not effective enough. The time series forecasting is essentially a regression task with continuous inputs, which clearly differs from classification tasks in NLP with discrete inputs. Accordingly, the canonical Autoregressive (AR) decoding cannot effectively handle the time series processing problem, mainly because the predictions of the previous $n - 1$ steps are not able to sufficiently avoid errors so that the n -th step is conditioned on predictions with high accumulative errors, leading to unsatisfactory final prediction performance. Besides, the encoder-only methods are simple variants of the AR decoding methods, utilizing the encoder of Transformer as a feature extractor and a Multi-Layer Perceptron (MLP) or a Convolution Layers Block as the decoder. Although this type of methods can eliminate accumulative errors to some extent, it fails to benefit from the powerful attention mechanisms. Secondly, diverse time series data typically has strong spatial dependencies, such as

traffic flows and skeleton-based action sequences. As shown in Figure 1(b), previous works, in exploring the modelling of both spatial and temporal dependencies in Transformer architecture, could be divided into two categories based on the their distinct manners of connecting spatial and temporal information (i.e. a parallel or a stacked manner). The parallel manner extracts spatial and temporal features separately and then aggregates them (Plizzari et al., 2020; Aksan et al., 2020). Whereas the stacked manner deals with the temporal and spatial dependencies alternately (Xu et al., 2020). As far as we are concerned, neither of them integrally considers the spatial and temporal dependencies for a joint modeling, as the temporal dependencies are ignored during the learning and prediction of spatial attentions and vice versa.

In this work, to address the above-mentioned challenging limitations, we present a new spatial-temporal Transformer for the time series forecasting problem. First of all, we design a Non-Autoregressive (Non-AR) Transformer architecture with a proposed Query Generation Block (QGB) embedded as a core module for the problem. QGB produces queries within one step, with the queries owning the same length as the target sequences. Then, utilizing the generated queries, our spatial-temporal Transformer decoder is able to perform forecasting parallelly. By so doing, not only the accumulative errors can be greatly avoided, but also the decoder can more effectively benefit from attention mechanisms. Moreover, in contrast to the existing parallel and stacked manners, we propose a novel spatial-temporal attention mechanism to jointly model the spatial and temporal dependencies in an integral manner. We first embed the input features into a high dimensional tensor, and predict the spatial and temporal attention maps along both space and time. Then, we perform a transposition on the temporal attention map to obtain a *temporal influence map*, which is further used to conduct a product operation with the spatial attention, resulting in a jointly learned integral spatial-temporal attention map.

Considering the ego-centric future localization as a case study, we validate our model on the NuScenes (Caesar et al., 2020) and a self-collected SMARTS-EGO dataset. The experimental results clearly demonstrate that our approach can achieve superior time-series forecasting performance and can remarkably reduce the decoding time. From both perspectives, our approach also outperforms state-of-the-art RNN-based and canonical Transformer models.

In summary, our contribution is three-folds:

- To the best of our knowledge, this is the first attempt to propose a Non-Autoregressive Transformer model for time series forecasting, generating total decoder queries within one step and enabling forecasting parallelly.
- We design a novel spatial-temporal attention mechanism,

building a bridge by a *temporal influence map* to integrally connect spatial and temporal attentions, so that spatial and temporal dependencies can be handled in a joint manner.

- We verify the model effectiveness on two competitive ego-centric future localization benchmarks, achieving state-of-the-art performance on both real-time and accuracy.

2. Related Work

We review the closely related works from three aspects, i.e. Non-Autoregressive Transformer models designed for the NLP task, spatial-temporal Transformer architectures, and Transformer models for time series forecasting.

2.1. Non-Autoregressive Transformer for NLP

Most previous Non-Autoregressive Transformer models aim at dealing with NLP tasks instead of the time series forecasting problem. Gu et al. (2018) propose a first Non-Autoregressive Transformer model, in which all the queries are obtained simultaneously by copying source inputs with learnable fertilities. With a condition on the sequence fertilities, the decoding process is thus non-autoregressive. Guo et al. (2019a) attempt to translate source sequences into target ones, aiming at enhancing the queries of decoder. Kasai et al. (2020) design Disentangled Context (DisCo) Transformer, which is able to produce all tokens simultaneously considering different contexts. Bao et al. (2019) stress the importance of position modeling in no-autoregressive text generation, thus presenting a non-autoregressive transformer via position learning to incorporate positions as latent variables into the text generation process. Ma et al. (2019) introduce latent variable models to non-autoregressive sequence generation to model complex distributions by generative flow technique. Qian et al. (2020) present Glancing Transformer (GLAT) with a glancing language model (GLM) to capture the word dependency gradually. However, none of these works explored the time-series forecasting problem via non-autoregressive modelling in the Transformer framework.

2.2. Spatial-Temporal Transformer

Spatial-temporal transformer architectures have been recently investigated by researchers to effectively utilize the spatial-temporal information in the modeling. Guo et al. (2019b) propose attention-based spatial-temporal graph convolutional networks (ASTERN), in which the attention mechanism is employed to capture the dynamic correlations and the graph convolution is applied to learn the spatial and temporal features. Xu et al. (2020) design a variant of the graph neural network, named Spatial Transformer, which is used together with the original Temporal Transformer for building temporal dependencies across long-range time

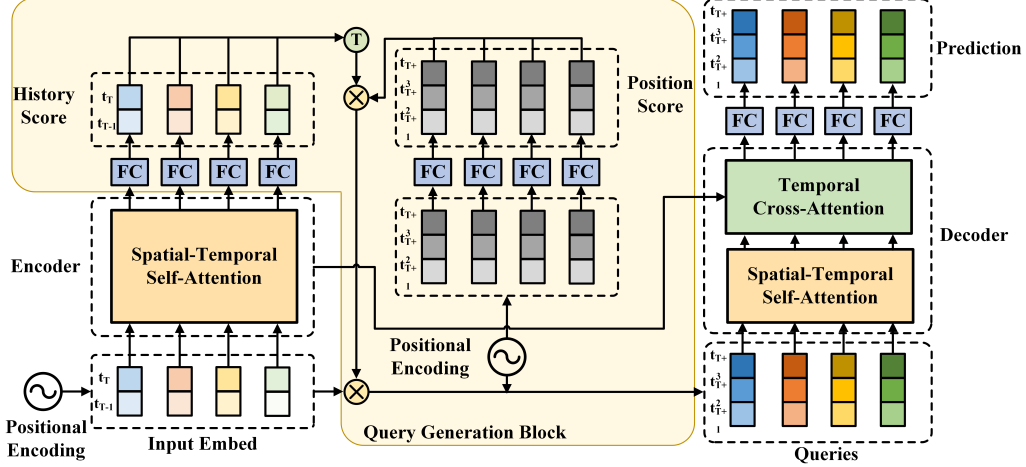


Figure 2. Illustration of the architecture of the proposed Non-Autoregressive Spatial-Temporal Transformer (NAST). Compared with the canonical Transformer, a Query Generation Block (QGB) is inserted between the encoder and decoder. The self-attention in the encoder and decoder is modelled and learned with a novel spatial-temporal attention mechanism to process the spatial and temporal dependencies integrally. The FC denotes Fully-Connected network.

steps. In Aksan et al. (2020), a Transformer-based architecture is adapted for generative modeling of 3D human motion which explicitly copes with the comprehensive spatial and temporal information in the task. Plizzari et al. (2020) attempt to use a two-stream spatial temporal Transformer network for skeleton-based action recognition. Yu et al. (2020) use only attentions to handle the problem of pedestrian trajectory prediction. They also introduce a read-writable external memory module ensuring the memory can be consistently updated by the temporal Transformer. Although promising performance has been achieved in these works, none of them considers combining non-autoregressive modeling with joint spatial-temporal attention learning in a unified Transformer architecture for robust time-series forecasting.

2.3. Transformer for Time Series Forecasting

There are only a very few fundamental studies in the literature on time series forecasting with Transformer models. As far as we know, Li et al. (2019) conduct the first study by adapting the Transformer model to time series forecasting, which surpasses the RNN-based methods on various performance metrics. The method produces queries and keys with causal convolution to incorporate local context into attention mechanism. However, the model and its variant proposed by Lin et al. (2020) only use the Transformer as the encoder, and the decoder simply employs an MLP instead of the original autoregressive decoder, causing an issue of requiring the same length for outputs and inputs. Wu et al. (2020) directly apply the vanilla canonical Transformer model to the time series forecasting, which regards the forecasting of next step as query and the decoder performs in an *autoregressive* manner. Our work is significantly

different from these existing time-series forecasting models by proposing a new *non-autoregressive* spatial-temporal transformer architecture for the task.

3. Background

3.1. Attention-based model

The Transformer model (Vaswani et al., 2017) is an encoder-decoder architecture that employs attention mechanisms as non-local operations and is originally designed for the machine language translation tasks. We review the technical details of Transformer as follows.

3.1.1. ATTENTION MECHANISM

For each word embedding e_i in a set E with $E = \{e_1, \dots, e_n\} \subset \mathbb{R}^{d_e}$, a query $q_j \in \mathbb{R}^{d_q}$, a key $k_i \in \mathbb{R}^{d_k}$ and a value vector $v_i \in \mathbb{R}^{d_v}$ are respectively calculated by a linear transformation from the embeddings, where d_e, d_q, d_k, d_v denote embedding dimensions. The attention weight of each word is then obtained by performing scaled dot-product and softmax normalization operations. The attention weight is then used to conduct a weighted summation over the values, yielding an attention-guided embedding. Such process can be written as follows:

$$\text{Attention}(Q, K, V) = \text{softmax} \left(\frac{QK^T}{\sqrt{d_k}} \right) V \quad (1)$$

where Q, K, V are the query, key, and value matrices, respectively. The division by $\sqrt{d_k}$ is performed in order to make the variance of the dot-product insensitive to the feature size.

Additionally, as Vaswani et al. (2017) mentioned, in order to

introduce the order information of the sequence, a positional encoding is added to the input embedding. The positional encoding is defined as follows:

$$E_{\text{pos}}(x, i) = \begin{cases} \sin\left(\frac{x}{1000^{i/d_e}}\right), & \text{if } i \equiv 0 \pmod{2} \\ \cos\left(\frac{x}{1000^{(i-1)/d_e}}\right), & \text{if } i \equiv 1 \pmod{2} \end{cases} \quad (2)$$

where x is the position of an item in the sequence, and i is the dimension of the encoding vector.

3.1.2. CANONICAL TRANSFORMER ARCHITECTURE

The canonical Transformer is a typical encoder-decoder architecture. The Encoder is a stack of several encoding layers, and each of them is composed of a self-attention block and a position-wise fully-connected feed-forward block. Decoder is a stack of several decoding layers consisting of three sub-blocks. In addition to the two sub-blocks with the same as those in the encoder layer, a cross-attention block is inserted into the decoder layer to learn the attention between the encoder outputs and decoder inputs (i.e. queries).

3.2. Problem Formulation

Ego-centric future localization is originally utilized for predicting pedestrians' future locations (Bhattacharyya et al., 2018; Yagi et al., 2018) and then introduced to autonomous driving (Yao et al., 2019a;b; Makansi et al., 2020). This problem can be formulated as follows. Let us denote the current time step as t_0 . Since T_h time-steps ago, a vehicle-mounted camera has observed a sequence of images. A multi-object tracking algorithm is assumed to be applied to this sequence, producing a set of bounding boxes $\mathbf{U}_h \in \mathbb{R}^{T_h \times N_o \times 4}$, where N_o is the total count of tracked objects in the sequence. Each bounding box is denoted as $u_h^{(t,i)} = (\mathbf{U}_h)_{ti} \triangleq ((u_h)_{x_1}^{(t,i)}, (u_h)_{y_1}^{(t,i)}, (u_h)_{x_2}^{(t,i)}, (u_h)_{y_2}^{(t,i)})$, where t is the time step, i is the object ID, $(u_h)_{x_1}, (u_h)_{y_1}, (u_h)_{x_2}, (u_h)_{y_2}$ are the x and y coordinates of the top-left and bottom-right points of the bounding box, respectively. The future localization problem is to forecast a set of the future bounding boxes $\mathbf{U}_f \in \mathbb{R}^{T_f \times N_o \times 4}$ of the observed objects in T_f time-steps based on \mathbf{U}_h .

4. Method

4.1. Overview

We now explain the proposed Non-Autoregressive Spatial-Temporal Transformer (NAST) in detail. As shown in Figure 2, we improve the canonical Transformer architecture to adapt to the time series forecasting task in two ways.

Firstly, we insert a QGB (see Sec. 4.2 for more details) between the encoder and decoder. This block takes the

encoder output, query positional encoding and input embedding as input, and yields total queries within one step. Benefiting from this design, the decoder is able to generate the forecasting parallelly.

Secondly, we replace the self-attention block in both encoder and decoder with a novel spatial-temporal attention block (see Sec. 4.3 for more details) to process the spatial and temporal dependencies integrally. In this block, we first embed the input features into a high dimensional tensor, and predict the spatial and temporal attention maps along both space and time. Then, we perform a transposition on the temporal attention map to obtain a *temporal influence map*, which is further used to conduct a product operation with the spatial attention. Hence, the final result exactly is a jointly learned integral spatial-temporal attention map.

4.2. Non-AR QGB

The *queries* play an important role in Transformer models. In machine language translation task, the *queries* are an additional target language sequence. However, in time series forecasting, since no additional sequences are used as input, Wu et al. (2020) take the predictions of the previous $n-1$ steps as the *queries* to predict for the n -th step. As previously mentioned, this autoregressive manner may introduce huge accumulative error and the inference cannot be parallelly performed. Inspired by Gu et al. (2018), we design a novel Query Generation Block (QGB) to produce the *queries* within one step, as shown in Figure 2. The detailed procedure is described as follow.

Initially, for each object O_n , $n \in N_o$, the *history score* $H^{(n)} \in \mathbb{R}^{T_h \times 1}$ is calculated according to the encoder outputs $E_{\text{out}}^{(n)} \in \mathbb{R}^{T_h \times d_{\text{model}}}$, representing the influence of the input sequence on the *queries*, where d_{model} denotes the embedding dimensions:

$$H^{(n)} = \max(0, E_{\text{out}}^{(n)} W_H + b_H) \quad (3)$$

Then, different from machine translation tasks, the prediction length of time series forecasting is known in advance, which means the length of *queries* is determined. In this case, we can obtain a *position score* $P^{(n)} \in \mathbb{R}^{T_f \times 1}$ based on the query positional encoding $E_{\text{pos}}^{(n)} \in \mathbb{R}^{T_f \times d_{\text{model}}}$, reflecting the positional influence on the *queries* (Note that the $P^{(n)}$ is the same for all objects):

$$P^{(n)} = \max(0, E_{\text{pos}}^{(n)} W_P + b_P) \quad (4)$$

Next, synthesizing the above two types of influence, the dot-product of $H^{(n)}$ and $P^{(n)}$ can be utilized as linear transformation weights of input embedding $E_{\text{in}}^{(n)} \in \mathbb{R}^{T_h \times d_{\text{model}}}$, and the *queries* $Q^{(n)} \in \mathbb{R}^{T_f \times d_{\text{model}}}$ is:

$$Q^{(n)} = P^{(n)} H^{(n) \text{T}} E_{\text{in}}^{(n)} \quad (5)$$

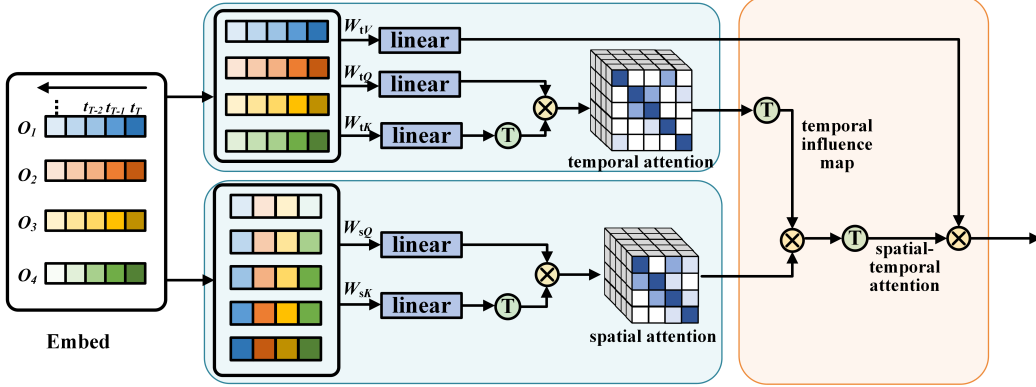


Figure 3. The Spatial-Temporal Attention Block. In this block, the spatial and temporal attention maps are predicted along both space and time of input features. Then, a transposition on the temporal attention map is operated to obtain a *temporal influence map*, which is further used to conduct a product operation with the spatial attention, resulting in a jointly learned spatial-temporal attention map.

Additionally, $W_P, W_H \in \mathbb{R}^{d_{\text{model}} \times 1}$, $b_P, b_H \in \mathbb{R}^{1 \times 1}$ are learnable parameters.

4.3. Spatial-Temporal Attention Block

The computing process of this block is illustrated in Figure 3 and we describe the details as follow.

Firstly, the spatial and temporal attention weights are calculated based on the original attention, respectively. In consideration of a high dimensional embedding $\mathbf{E} \in \mathbb{R}^{T_t \times N_o \times d_{\text{model}}}$, when process spatial attention, the time dimension is viewed as a batch dimension and the canonical attention mechanism is applied independently to each time step. Once temporal attention is needed to apply, we transpose the order of temporal and spatial dimension, view the spatial dimension as a batch dimension and perform the same attention operation as before. Note that for temporal attention, the positional encoding of canonical Transformer (Equation 2) is added to *query* and *key*. As for spatial attention, since in our consideration all objects constitute a position-independent undirected graph, no positional encoding would be added. More formally, regarding temporal attention, for each object $O_n, n \in N_o$, the attention along the time dimension can be calculated as:

$$E_t^{(n)} = E^{(n)} = \mathbf{E}_{\cdot \cdot n}, \quad (6)$$

$$Q_t^{(n)} = K_t^{(n)} = E_t^{(n)} + E_{\text{pos}}^{(n)}, \quad (7)$$

$$V_t^{(n)} = E_t^{(n)}, \quad (8)$$

$$A_t^{(n)} = \text{softmax} \left(\frac{(Q_t^{(n)} W_{tQ})^T (K_t^{(n)} W_{tK})}{\sqrt{d_{\text{model}}}} \right) \quad (9)$$

Regarding spatial attention, for each time step $t \in T_t$, the

attention for all objects can be calculated as:

$$E_s^{(t)} = E^{(t)} = \mathbf{E}_{t \cdot \cdot}, \quad (10)$$

$$Q_s^{(t)} = K_s^{(t)} = E_s^{(t)}, \quad (11)$$

$$A_s^{(t)} = \text{softmax} \left(\frac{(Q_s^{(t)} W_{sQ})^T (K_s^{(t)} W_{sK})}{\sqrt{d_{\text{model}}}} \right) \quad (12)$$

where $W_{sQ}, W_{sK}, W_{tQ}, W_{tK}, W_{tV} \in \mathbb{R}^{d_{\text{model}} \times d_{\text{model}}}$ are all learnable parameters. To represent the spatial attention over all time steps in a tensor, all the spatial attention weights $\{A_s^{(t)} | t = 1, 2, \dots, T_t\}$ are packed together into $\mathbf{A}_s \in \mathbb{R}^{T_t \times N_o \times N_o}$, where $(\mathbf{A}_s)_{t \cdot \cdot} = A_s^{(t)}$. Similarly, $\mathbf{A}_t \in \mathbb{R}^{N_o \times T_t \times T_t}$, where $(\mathbf{A}_t)_{n \cdot \cdot} = A_t^{(n)}$, is the packed temporal attention, representing the temporal attention for all objects. Additionally, all the $\{V_t^{(n)} | n = 1, 2, \dots, N_o\}$ is also packed into $\mathbf{V}_t \in \mathbb{R}^{T_t \times N_o \times d_{\text{model}}}$, where $(\mathbf{V}_t)_{\cdot n} = V_t^{(n)}$.

Secondly, indexing the temporal attention tensor \mathbf{A}_t by the last time dimension can generate the attention weights $A_t''^{(t)} = (\mathbf{A}_t)_{\cdot \cdot t} \in \mathbb{R}^{N_o \times T_t}$, which is termed as a *temporal influence map*, representing the temporal influence of time step t on each object. Then, we formulate the influenced spatial attention $A_{\text{st}}^{*(t)}$ as the product of $A_s^{(t)}$ and $A_t''^{(t)}$:

$$A_{\text{st}}^{*(t)} = A_s^{(t)} A_t''^{(t)} \quad (13)$$

Thirdly, all the $\{A_{\text{st}}^{*(t)} | t = 1, 2, \dots, T_t\}$ are packed into $\mathbf{A}_{\text{st}}^* \in \mathbb{R}^{T_t \times N_o \times T_t}$, where $(\mathbf{A}_{\text{st}}^*)_{t \cdot \cdot} = A_{\text{st}}^{*(t)}$. To match the size of each dimension of \mathbf{V}_t , we transpose the first and second dimension of \mathbf{A}_{st}^* , of which the result $\mathbf{A}_{\text{st}} \in \mathbb{R}^{N_o \times T_t \times T_t}$ is named as *spatial-temporal attention*.

Finally, for each object $O_n, n \in N_o$, the output embedding $E_{\text{out}}^{(n)}$ is calculated as the product of $A_{\text{st}}^{*(n)}$ and $V_t^{(n)}$:

$$E_{\text{out}}^{(n)} = A_{\text{st}}^{*(n)} V_t^{(n)} \quad (14)$$

4.4. Network Optimization

In order to train the model, we deploy the Smooth L1 Loss L_{1s} proposed by Girshick (2015) as the loss function to supervise the coordinate distance between the bounding boxes of the current and the future time steps. For each object, Let us denote the prediction as $\mathbf{Z} \in \mathbb{R}^{T_f \times N_o \times 4}$ and the ground truth as $\mathbf{G} \in \mathbb{R}^{T_f \times N_o \times 4}$. For each object O_n ($n \in N_o$) and each time step $t \in T_t$, $z^{(t,i)} = \mathbf{Z}_{ti}, g^{(t,i)} = \mathbf{G}_{ti}$, the optimization loss L_o can be formulated as:

$$L^{(t,i)}(z^{(t,i)}, g^{(t,i)}) = \sum_k L_{1s}(g_k^{(t,i)}, z_k^{(t,i)}) \quad (15)$$

Where $k = \{x_1, y_1, x_2, y_2\}$ representing the bounding box coordinates. Then the overall optimization loss is the sum of all $L^{(t,i)}$:

$$L_o = \sum_t \sum_i L^{(t,i)} \quad (16)$$

5. Experiments

5.1. Datasets

NuScenes Known as a huge autonomous driving dataset, the nuScenes (Caesar et al., 2020) contains 1000 scenes and each of them owns 20 seconds. Notably, it provides accurate bounding box trackings for different types of traffic objects. Herein, we select the nuScenes to train and evaluate the efficacy and performance of our proposed framework. The training/validation split is 700/150 scenes. The tracking bounding box annotated on key frames is adapted to train and test our model.

SMARTS-EGO Given that only the key frames (two frames per second) are annotated in NuScenes, the length of sequences is not enough to validate our model. Thus, we use SMARTS (Zhou et al., 2020) simulator to generate a large-scale ego-centric future localization dataset named SMARTS-EGO, which contains 7700 scenes and each of them own 10 seconds. The frame rate is 10 and all frames have the ground truth of bounding box trackings for traffic objects generated by the simulator. We randomly split the dataset into 6200 scenes for training and 1500 for validation.

5.2. Metrics

In order to evaluate the performance of our model, we adopt three metrics described as follow.

ADE The Displacement Error (DE) is the L2 distance between the centers of the forecasted and ground-truth bounding box. The Average Displacement Error (ADE) is the average of DE from the current time step till the final ones. This metric is utilized to estimate the average error over the whole forecasting process.

FDE The Final Displacement Error (FDE) is the DE at

the final time step, the metric of which is used to assess the accumulative error.

FIOU The Final Intersection Over Union (FIOU) is the IOU between the forecasted and ground-truth bounding box at the final time step. This metric is able to reflect a synthetical forecasting accuracy of the top-left and bottom-right coordinates of bounding box.

5.3. Training Details

Our experiments are all performed on a workstation with Ayzen R3900X CPU and Nvidia RTX 3090 GPU. The implement of the Transformer architecture follows this set, in which the number of the parallel attention layer in a *multi-head attention* is set to 1, the dimensions of embedding features is set to 64, and the sub-layers in both encoder and decoder are stacked for four times.

While training, we choose Adam (Kingma & Ba, 2015) as the optimizer and set the batch size to 16 for SMARTS-EGO and 64 for NuScenes. We use a learning rate variation strategy according to Vaswani et al. (2017) as follows:

$$lrate = d_{\text{model}}^{-0.5} \cdot \min(\text{step_num}, \text{step_num} \cdot \text{warmup_step}^{-1.5}) \quad (17)$$

In our experiments, *warmup_step* is set to 5000,

As for dataset, the frame rate is 2 and 10 in NuScenes and SMARTS-EGO, respectively. Additionally, for both the two datasets, the width and height of a frame is resize to 512 and 320.

5.4. Ablation Studies

Aiming at validating the performance of the Non-AR decoding method and spatial-temporal attention mechanism, we conduct a series of ablation studies. The results and discussion are as follow.

5.4.1. ABLATION STUDIES ABOUT NON-AR DECODING METHOD

To validate the performance of different decoding methods, we replace the Non-AR decoding of our NAST model with two typical methods mentioned in Figure 1(a), including the AR method and MLP method. Apart from this, the other settings of the three models are all the same.

For the purpose of evaluating the performance of the three models on different length of time series, we choose four pairs of (T_h, T_f) , including (1.5s, 1.5s), (1.5s, 3s), (3s, 3s) and (3s, 4.5s). As mentioned in Sec. 5.3, the pairs of historical and future sequence length of SMARTS-EGO are (15, 15), (15, 30), (30, 30) and (30, 45), while those of NuScenes are (4, 3), (4, 6), (7, 6) and (7, 9)(the current

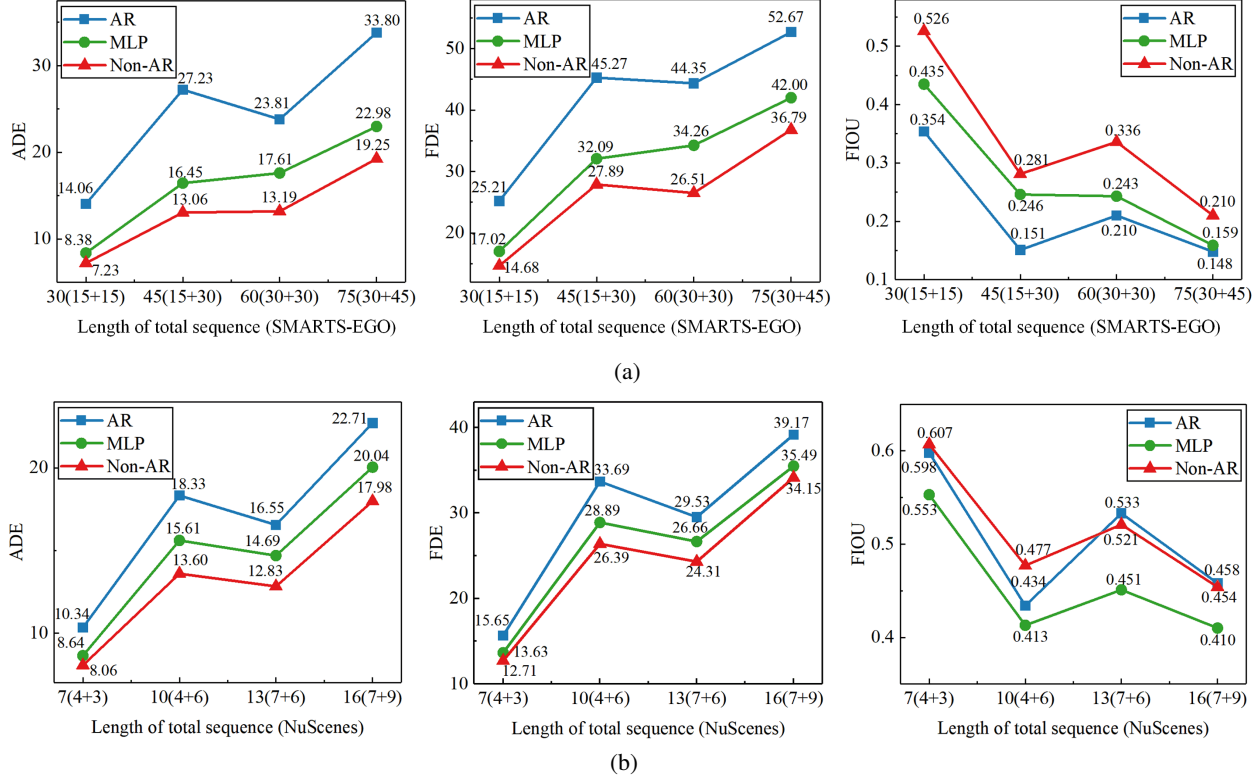


Figure 4. (a) The evaluating results of the three decoding methods (AR, MLP and Non-AR) on SMARTS-EGO dataset. (b) The evaluating results of the three decoding methods (AR, MLP and Non-AR) on NuScenes dataset. (AR: Autoregressive; Non-AR: Non-Autoregressive; MLP: Multi-Layer Perceptron; ADE: Average Displacement Error; FDE: Final Displacement Error; FIOU: Final Intersection Over Union)

frame is included in the historical sequence).

The evaluating results of the three decoding methods on SMARTS-EGO and NuScenes datasets are illustrated in Figure 4(a) and Figure 4(b), respectively. As the results shown, the AR decoding method performs acceptably on NuScenes dataset where the sequence is not too long. Once the sequence become longer in SMARTS-EGO, severe degradation of the performance would occur because of the accumulative error. In contrast, the MLP method suffers little from the accumulative errors and performs well on both SMARTS-EGO and NuScenes. Moreover, benefiting from the attention mechanism, the Non-AR decoding outperforms far beyond MLP on both two datasets, no matter how long the sequence is. The results prove that the Non-AR decoding method cannot only avoid the huge accumulative error, but also profit from the attention mechanism.

5.4.2. ABLATION STUDIES ABOUT SPATIAL-TEMPORAL MECHANISM

Similarly, to validate the performance of the spatial-temporal mechanism, we replace this attention block of our NAST model with various types of architectures, mentioned in Figure 1(b) including the canonical manner, the parallel manner and stacked manner. More specifically, for the parallel manner, we implement a *parallel spatial temporal*

block, which deals with the spatial and temporal attention respectively and then aggregates the information by “sum” or “concatenate” operation. This block is stacked for four times in both encoder and decoder. As for the stacked manner, we choose two kinds of stacked orders, each of which contains four temporal attention blocks and four spatial attention blocks. Results and more details are shown in Table 1.

As the results shown, the manners of modeling the spatial and temporal attention have significant influence on the performance. In terms of the parallel manner, the “concatenate” operation of aggregation performs better than “sum” on both SMARTS-EGO and NuScenes. And with regard to the stacked manner, different orders make a noticeable impact and the unbefitting order even degrades the performance, which needs more cautious design and lots of trial and error. However, without additional architecture design and aggregate operation, replacing the original attention block with spatial-temporal attention can outperform all the other manners. The results stress that the spatial-temporal mechanism is applicable and effective for time series forecasting.

5.5. Compare with State-of-the-Arts

To assess the performance, we compare our proposed model with one RNN-based model and two Transformer-based models that represent various state-of-the-art methods.

Table 1. The ablation studies about the spatial-temporal attention on SMARTS-EGO and NuScenes Datasets ($(T_h=1.5$ s, $T_f=1.5$ s)). (T: Temporal attention block; S: Spatial attention block; TS: Spatial-temporal attention block; *||*: the parallel connection; (*, *): the stacked connection; SUM: aggregate by “sum”; CAT: aggregate by “concatenate”)

TYPES	BLOCKS	SMARTS-EGO			NUSCENES		
		ADE \downarrow	FDE \downarrow	FIOU \uparrow	ADE \downarrow	FDE \downarrow	FIOU \uparrow
CANONICAL	(T, T, T, T)	7.85	16.17	0.408	8.29	12.92	0.585
PARALLEL	(T S, T S, T S, T S) – SUM	8.78	16.91	0.387	8.86	13.77	0.564
	(T S, T S, T S, T S) – CAT	7.95	16.24	0.465	8.08	12.70	0.596
STACKED	(T, S, T, S, T, S, T, S)	7.76	15.88	0.420	8.39	13.28	0.581
	(S, T, S, T, S, T, S, T)	7.98	16.25	0.420	8.37	13.15	0.567
OURS	(TS, TS, TS, TS)	7.23	14.68	0.526	8.06	12.71	0.607

Table 2. Compare our method with state-of-the-arts with different T_h and T_f on SMARTS-EGO and NuScenes Datasets.

METHOD	T(s)		SMARTS-EGO			NUSCENES		
	T_h	T_f	ADE \downarrow	FDE \downarrow	FIOU \uparrow	ADE \downarrow	FDE \downarrow	FIOU \uparrow
RNN-ED (YAO ET AL., 2019A)	1.5	1.5	7.68	15.55	0.508	7.850	12.48	0.584
	1.5	3	14.63	28.97	0.290	14.32	26.69	0.458
	3	3	15.59	30.25	0.285	13.21	24.29	0.516
	3	4.5	20.90	37.82	0.179	18.79	33.69	0.444
TRANSFORMER (WU ET AL., 2020)	1.5	1.5	14.12	25.62	0.358	20.45	29.05	0.436
	1.5	3	23.72	43.64	0.209	29.99	43.36	0.350
	3	3	26.34	45.61	0.209	26.89	38.63	0.432
	3	4.5	32.00	57.06	0.167	29.78	42.43	0.387
TST-NOLOGSPARSE (LI ET AL., 2019)	1.5	1.5	12.16	19.98	0.432	13.27	13.44	0.596
	1.5	3	-	-	-	-	-	-
	3	3	21.98	37.53	0.233	20.57	26.10	0.485
	3	4.5	-	-	-	-	-	-
NAST(OURS)	1.5	1.5	7.23	14.68	0.526	8.06	12.71	0.607
	1.5	3	13.06	27.89	0.281	13.60	26.39	0.477
	3	3	13.19	26.51	0.336	12.83	24.31	0.521
	3	4.5	19.25	36.79	0.210	17.98	34.15	0.454

RNN-ED RNN-ED proposed by Yao et al. (2019a) is a RNN-based encoder-decoder model. We remove the optical flow encoding branch of it and reserve all the other settings.

Transformer We follow the AR manner mentioned in Wu et al. (2020) to apply canonical Transformer to this task. Besides, other settings are the same as our model.

TST-NoLogSparse Time-Series Transformer (TST) is proposed by Li et al. (2019). The author only publishes the *NoSparse* version, thereby we validate only this in our task, with all the other settings the same as the origin.

As the results shown in Table 2, our model displays far better performance than other Transformer-based methods, and achieves remarkable performance superior to RNN-based method. Especially, with the increasing of the length of sequences, more prominent superiority of our model over RNN-based method is observed, suggesting the immense

potential of NAST to handle the time series forecasting.

6. Conclusions

In this paper, we propose a Non-Autoregressive Transformer decoding and design a novel spatial-temporal attention mechanism to handle spatial and temporal attentions in a joint manner. This is the first attempt to introduce a Non-autoregressive Transformer model into time series forecasting with spatial and temporal dependencies. Experimentally, the results demonstrate that both of the spatial-temporal attention mechanism and non-autoregressive decoding manner are necessary and beneficial. Accordingly, our model outperforms far better than other Transformer-based methods, and achieves effective performance superior to RNN-based methods. For future work, our model can be a solid baseline for the time series forecasting with Transformer. Meanwhile, more explainable methods to generate queries and model the spatial-temporal attentions are still of urgent needs.

References

Aksan, E., Cao, P., Kaufmann, M., and Hilliges, O. Attention, please: A spatio-temporal transformer for 3d human motion prediction. *arXiv preprint arXiv:2004.08692*, 2020.

Bao, Y., Zhou, H., Feng, J., Wang, M., Huang, S., Chen, J., and Li, L. Non-autoregressive transformer by position learning. *arXiv preprint arXiv:1911.10677*, 2019.

Bhattacharyya, A., Fritz, M., and Schiele, B. Long-term on-board prediction of people in traffic scenes under uncertainty. In *CVPR*, 2018.

Brown, T. B., Mann, B., Ryder, N., Subbiah, M., Kaplan, J., Dhariwal, P., Neelakantan, A., Shyam, P., Sastry, G., Askell, A., Agarwal, S., Herbert-Voss, A., Krueger, G., Henighan, T., Child, R., Ramesh, A., Ziegler, D. M., Wu, J., Winter, C., Hesse, C., Chen, M., Sigler, E., Litwin, M., Gray, S., Chess, B., Clark, J., Berner, C., McCandlish, S., Radford, A., Sutskever, I., and Amodei, D. Language models are few-shot learners. In Larochelle, H., Ranzato, M., Hadsell, R., Balcan, M., and Lin, H. (eds.), *NeurIPS*, 2020.

Caesar, H., Bankiti, V., Lang, A. H., Vora, S., Lioung, V. E., Xu, Q., Krishnan, A., Pan, Y., Baldan, G., and Beijbom, O. nuscenes: A multimodal dataset for autonomous driving. In *CVPR*, 2020.

Carion, N., Massa, F., Synnaeve, G., Usunier, N., Kirillov, A., and Zagoruyko, S. End-to-end object detection with transformers. In *ECCV*, 2020.

Dai, Z., Yang, Z., Yang, Y., Carbonell, J. G., Le, Q. V., and Salakhutdinov, R. Transformer-xl: Attentive language models beyond a fixed-length context. In *ACL*, 2019.

Girshick, R. Fast r-cnn. In *ICCV*, 2015.

Gu, J., Bradbury, J., Xiong, C., Li, V. O. K., and Socher, R. Non-autoregressive neural machine translation. In *ICLR*, 2018.

Guo, J., Tan, X., He, D., Qin, T., Xu, L., and Liu, T.-Y. Non-autoregressive neural machine translation with enhanced decoder input. In *AAAI*, 2019a.

Guo, S., Lin, Y., Feng, N., Song, C., and Wan, H. Attention based spatial-temporal graph convolutional networks for traffic flow forecasting. In *AAAI*, 2019b.

Huang, C. A., Vaswani, A., Uszkoreit, J., Simon, I., Hawthorne, C., Shazeer, N., Dai, A. M., Hoffman, M. D., Dinculescu, M., and Eck, D. Music transformer: Generating music with long-term structure. In *ICLR*, 2019.

Karim, F., Majumdar, S., Darabi, H., and Chen, S. Lstm fully convolutional networks for time series classification. *IEEE Access*, 6:1662–1669, 2018. doi: 10.1109/ACCESS.2017.2779939.

Kasai, J., Cross, J., Ghazvininejad, M., and Gu, J. Non-autoregressive machine translation with disentangled context transformer. In *ICML*, 2020.

Kingma, D. P. and Ba, J. Adam: A method for stochastic optimization. In Bengio, Y. and LeCun, Y. (eds.), *ICLR*, 2015.

Li, S., Jin, X., Xuan, Y., Zhou, X., Chen, W., Wang, Y.-X., and Yan, X. Enhancing the locality and breaking the memory bottleneck of transformer on time series forecasting. In *NeurIPS*, 2019.

Lin, Y., Koprinska, I., and Rana, M. Springnet: Transformer and spring dtw for time series forecasting. In *ICONIP*, 2020.

Liu, Z., Luo, S., Li, W., Lu, J., Wu, Y., Li, C., and Yang, L. Convtransformer: A convolutional transformer network for video frame synthesis. *arXiv preprint arXiv:2011.10185*, 2020.

Ma, X., Zhou, C., Li, X., Neubig, G., and Hovy, E. Flowseq: Non-autoregressive conditional sequence generation with generative flow. In *EMNLP-IJCNLP*, 2019.

Makansi, O., Cicek, O., Buchicchio, K., and Brox, T. Multi-modal future localization and emergence prediction for objects in egocentric view with a reachability prior. In *CVPR*, 2020.

Plizzari, C., Cannici, M., and Matteucci, M. Spatial temporal transformer network for skeleton-based action recognition. *arXiv preprint arXiv:2008.07404*, 2020.

Qian, L., Zhou, H., Bao, Y., Wang, M., Qiu, L., Zhang, W., Yu, Y., and Li, L. Glancing transformer for non-autoregressive neural machine translation. *arXiv preprint arXiv:2008.07905*, 2020.

Sagheer, A. and Kotb, M. Time series forecasting of petroleum production using deep lstm recurrent networks. *Neurocomputing*, 323:203 – 213, 2019. ISSN 0925-2312.

Vaswani, A., Shazeer, N., Parmar, N., Uszkoreit, J., Jones, L., Gomez, A. N., Kaiser, Ł., and Polosukhin, I. Attention is all you need. In *NeurIPS*, 2017.

Wu, N., Green, B., Ben, X., and O’Banion, S. Deep transformer models for time series forecasting: The influenza prevalence case. *arXiv preprint arXiv:2001.08317*, 2020.

Xu, M., Dai, W., Liu, C., Gao, X., Lin, W., Qi, G.-J., and Xiong, H. Spatial-temporal transformer networks for traffic flow forecasting. *arXiv preprint arXiv:2001.02908*, 2020.

Yagi, T., Mangalam, K., Yonetani, R., and Sato, Y. Future person localization in first-person videos. In *CVPR*, 2018.

Yao, Y., Xu, M., Choi, C., Crandall, D. J., Atkins, E. M., and Dariush, B. Egocentric vision-based future vehicle localization for intelligent driving assistance systems. In *ICRA*, 2019a.

Yao, Y., Xu, M., Wang, Y., Crandall, D. J., and Atkins, E. M. Unsupervised traffic accident detection in first-person videos. In *IROS*, 2019b.

Yu, C., Ma, X., Ren, J., Zhao, H., and Yi, S. Spatio-temporal graph transformer networks for pedestrian trajectory prediction. In *ECCV*, 2020.

Zhou, M., Luo, J., Villela, J., Yang, Y., Rusu, D., Miao, J., Zhang, W., Alban, M., Fadakar, I., Chen, Z., et al. Smarts: Scalable multi-agent reinforcement learning training school for autonomous driving. *arXiv preprint arXiv:2010.09776*, 2020.